Pendent Polyimides Using Mellitic Acid Dianhydride. III. The Effect of Pendent Group Functionality on Polymer Properties

Marvin L. Illingsworth,[1] Wei Wang,[1] Jonathan P. McCarney,[1] Kenneth A. Hughes,[1] Kari J. Trotter,[1] Russell A. Stapleton,[1] Jeffrey R. Chabot,[2] Emilie J. Siochi,[3] Michael Kotlarchyk[2]

[1]*Department of Chemistry, Rochester Institute of Technology, Rochester, New York 14623*
[2]*Department of Physics, Rochester Institute of Technology, Rochester, New York 14623*
[3]*NASA Langley Research Center, Hampton, Virginia 23681-0001*

Received 30 April 2008; accepted 2 January 2009
DOI 10.1002/app.29986
Published online 2 April 2009 in Wiley InterScience (www.interscience.wiley.com).

ABSTRACT: Methyl, methoxy, and nitrile (cyano) functional groups were incorporated into the metal–organic pendent group of a co-polyamic acid, co-PAA[(3,4′-ODA/ODPA)$_{0.9}$(3,4′-ODA/{MADA-*p*-Zr(adsp)(Rdsp)})$_{0.1}$], in various locations to investigate their effects on polymer chain interactions and film quality. Proton nuclear magnetic resonance and gel permeation chromatography (GPC) performed on solutions of these products were consistent with the expected 10% (mol) functionalized pendent polymeric structures. Thermogravimetric analysis performed on ether-precipitated samples revealed little functional group effect on imidization temperature (decreases of 5–8°C), but showed a somewhat-greater effect on decomposition temperature (decreases of 6°C for the 3-methoxy derivative to 28°C for the methyl derivative). Differential scanning calorimetry performed on imidized powder samples showed that glass transition temperatures increased with the addition of the functional groups from 2°C for the methyl derivative to 19°C for the 3-methoxy derivative. Imidized films were solvent resistant, transparent, and flexible, with the nitrile derivative least susceptible to crack formation. Light scattering results revealed that the nitrile derivative had the lowest second virial coefficient of the functional groups tested and formed aggregates at room temperature in NMP with $n = 2$, thus rationalizing its superior film forming properties. Results of contact angle measurements and atomic oxygen exposure of functionalized pendent co-PI films are included. © 2009 Wiley Periodicals, Inc. J Appl Polym Sci 113: 1198–1206, 2009

Key words: functionalization of polymers; polyimide; films; polymer chain interactions; atomic oxygen

INTRODUCTION

Understanding and controlling polymer chain interactions continues to be of fundamental importance in polymer science. Some of the relevant parameters investigated previously include polymer molecular weight,[1,2] temperature and solvent control of chain conformation,[3–9] the addition of ancillary polymers (blends) or small molecules,[10–15] main chain structural features (e.g., spiro structure,[16] pattern of ring substitution,[17] and block copolymer interactions[18,19]), degree of hydrogenation,[20] functionalization of endgroups (for design of supramolecular architectures),[21] and attachment/grafting of side groups onto polymer chains.[4,22–48]

Side group structures that have been used to control specific interchain interactions include electrically charged groups,[22–25] bulky/hydrophobic aliphatic groups,[4,26–35] mesogenic groups,[36,37] fluorinated groups,[38] alkoxy groups,[6,7,39,40] bridging groups,[33] and hydrogen-bonding/functional groups.[41–48] As a result, some of the structural features and properties that have been manipulated/enhanced include the degree of polymer chain aggregation,[24,25,28,37,39] charge transportation/luminescent intensity,[7,22,23,29,31–33,37,39,40] folding,[26] surface chain configuration as a function of the rate of solvent evaporation,[30] gelation,[27] miscibility,[42,47] crystallization (for crystal engineering),[46,48] chain orientation[36,37] (including liquid crystal formation),[37] magnetic dipole interactions,[38] film adhesion,[45] photo-oxidative damage,[7] filament morphologies,[34] and macromolecular recognition.[41,43,44] About 10 years ago, researchers in our laboratory began using metal-organic side groups to enhance polymer atomic oxygen (AO) resistance[49] and so have developed a similar interest.

Initially, to lengthen the useful life of polymeric materials in low earth orbit, metal-organic compounds were dissolved in polyamic acid (PAA)

Additional Supporting Information may be found in the online version of this article.

Correspondence to: M. L. Illingsworth (mlisch@rit.edu).

solutions. The PAA solutions chosen were precursors of space-qualified polyimides (PIs). Wet films were then cast and thermally imidized.[50] The in situ generation of a protective metal oxide layer upon land-based AO exposure was considered proof of concept.[50,51] However, a significant decrease in film quality was observed even at relatively low additive concentrations. To address this limitation, the structures of the PAAs[52–54] and of one of the additives[49] were modified so that they could be covalently attached, i.e., the metal-organic additive would now be a pendent group. As a result, substantial increases in the metal-organic mole percentage became possible (up to 50 mole percent) while retaining good film quality.[52] Recognizing the opportunity to better understand the structural parameters that affect polymer chain interactions and film formation, we elected to subtly modify the pendent groups with simple functional moieties of different polarities and at different locations. The use of limited concentrations of functional groups to control polymer chain interaction has not been extensively investigated.[36,47,55] We chose to use co-PAAs with 4,4′-ODA/ODPA and 3,4′-ODA/ODPA for this study because the structures of their homopolymers resemble those of Kapton™ and NASA's LARC-IA (Langley Research Center-Improved Adhesive),[56] respectively.

Thus, we wish to report: (i) the synthesis and characterization of four new pendent PAAs, co-PAA[(3,4′-ODA/ODPA)$_{0.9}$(3,4′-ODA/MADA-*p*-Zr(adsp)(Rdsp))$_{0.1}$], where the R group is 3-methoxy or 5-methoxy on the salicylidene rings, or 5-cyano (nitrile) or 5-methyl on the diamine ring (see Fig. 1), (ii) the solution casting of these polymers onto glass substrates, (iii) the thermal imidization of the wet films, and, (iv) the evaluation of the resulting pendent co-PI films, including crack formation, creasibility, solvent resistance, contact angles with water, and evidence of atomic oxygen resistance. In addition, laser light scattering was used to rationalize why the nitrile co-PAA polymer exhibited superior film forming ability as compared with the other functionalized pendent co-PAAs, and these results are included as well.

Experimental section

All starting materials and solvents were obtained from sources, handled, and purified as described previously.[52–54] MADA was prepared and its purity established by thermogravimetric analysis (TGA) as reported previously.[54] The nonfunctionalized pendent group precursor (4-amino-*N*,*N*′-disalicylidene-1,2-phenylenediaminato)(*N*,*N*′-disalicylidene-1,2-phenylenediaminato)zirconium(IV), Zr(adsp)(Rdsp) where R = H, and all functionalized precursors were prepared as previously reported.[49,57] The 50.1 percent yield obtained for the nitrile-substituted ligand, H_2cdsp, was significantly greater than that reported.[57]

Instruments and methods

Fourier transform infrared (FTIR) spectroscopy, nuclear magnetic resonance (NMR), TGA, differential scanning calorimetry (DSC) (all samples analyzed twice), gel permeation chromatography (GPC) in 0.02 M LiBr/NMP (performed at the NASA Langley Research Center), oxygen plasma ashing, and scanning electron microscopy data were obtained as before.[52–54] GPC was conducted with both a DRI and a differential viscosity (DV) detector. Polymer film samples were prepared, imidized, and evaluated (crack formation, creasibility, solvent resistance and atomic oxygen resistance) as described previously.[52–54]

Contact angle measurements were made with the use of water droplets on free-standing films using a Rame-Hart 100–00 115 instrument. Films of LARC-IA were made from powder samples with 3 percent offset at Eastman Kodak Co at 360°C under 10T and at 340°C under 5T.

Light scattering data for pendent co-PAA solutions in NMP were collected with the use of a Brookhaven Instruments BI-200SM goniometer equipped with a 35-mW, vertically polarized Model 127 Spectra-Physics He-Ne laser (wavelength, $\lambda = 632.8$ nm) and an EMI-9863 photomultiplier. Samples were contained in 12-mm O.D. round glass cells immersed in decahydronaphthalene index-matching fluid. For each sample type, light intensities were measured at a scattering angle of 90° (the angle between the scattered light and the incident beam propagation directions) for a series of approximately 6–9 concentrations ranging from approximately $c = 0.02$ g/cm^3 downward. The scattered intensities were converted to excess Rayleigh ratios[58] (R_{90}) by subtracting off the scattering from pure solvent and comparing the excess intensity to the 90° scattering from a pure toluene standard with known Rayleigh ratio at the laser wavelength. The polymer weight-average molecular weight, M_w, and second virial coefficient, A_2, were determined from a plot of KR_{90}/c vs. c. This is an alternate form of a Debye plot, and the data can be fitted to the linear form

$$\frac{R_{90}}{K_c} = M_w(1 - 2A_2M_wc). \quad (1)$$

Here, K is an optical constant defined by

$$K = \frac{2\pi^2 n_0^2}{\lambda^4 N_A}\left(\frac{dn}{dc}\right)^2, \quad (2)$$

where $n_0 = 1.47$ is the refractive index of the NMP solvent and N_A is Avogadro's number. The quantity

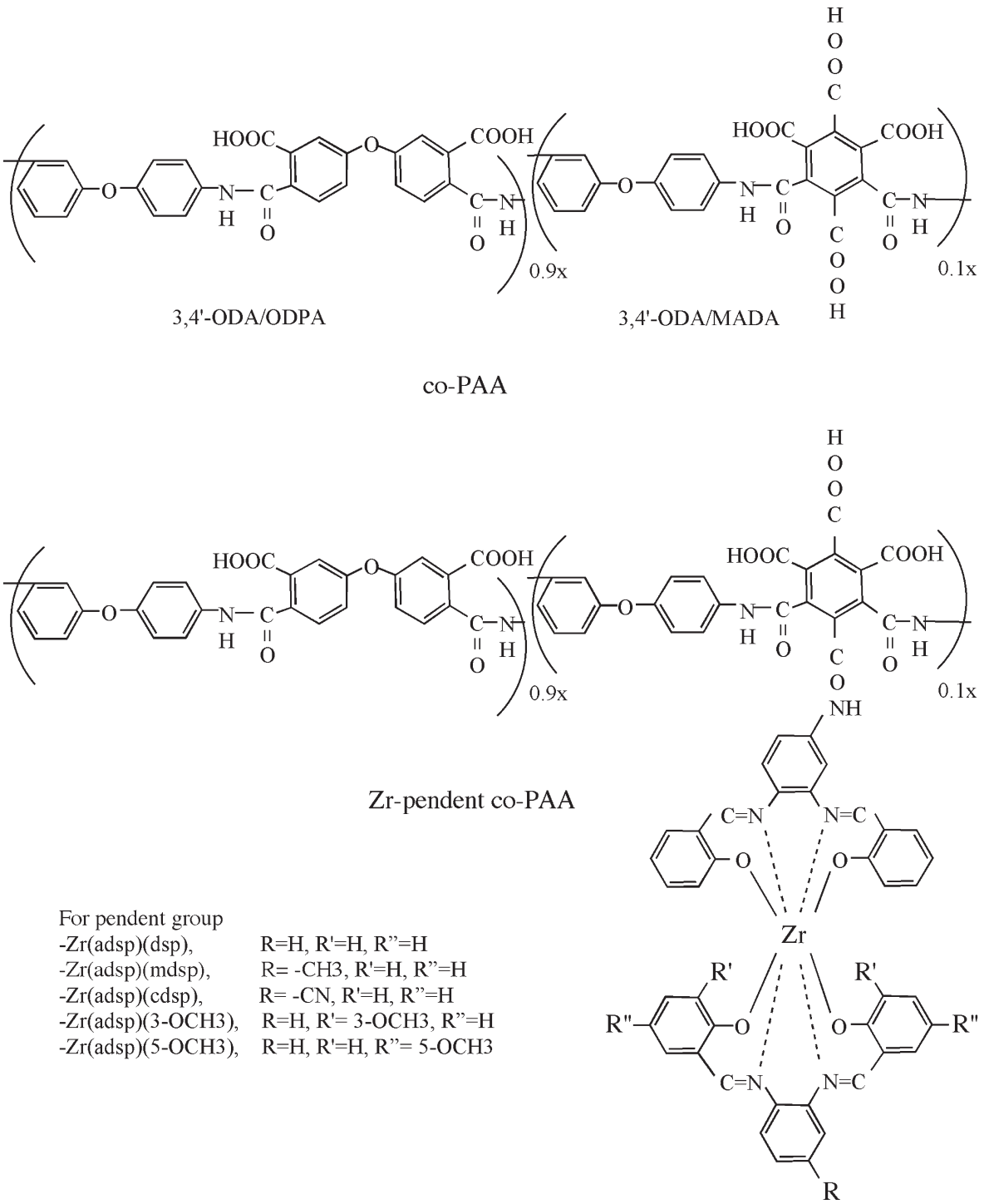

Figure 1 Nonpendent and Zr-pendent co-polyamic acids.

dn/dc is the differential refractive index increment and was measured with a Spectronic 334610 Refractometer.

Synthesis

Although the synthesis of co-poly[(4,4′-oxydiphthalic anhydride/4,4′-oxydianiline)$_{0.9}$(mellitic acid dianhydride/4,4′-oxydianiline)$_{0.1}$]amic acid, co-PAA[(OPDA/4,4′-ODA)$_{0.9}$(MADA/4,4′-ODA)$_{0.1}$], the Kapton-like nonpendent co-PAA, and co-poly[(4,4′-oxydiphthalic anhydride/3,4′-oxydianiline)$_{0.9}$(mellitic acid dianhydride/3,4′-oxydianiline)$_{0.1}$]amic acid, co-PAA[(OPDA/3,4′-ODA)$_{0.9}$(MADA/3,4′-ODA)$_{0.1}$], the LARC-IA-like nonpendent co-PAA, have been performed previously,[52,53] the description of a larger-scale preparation of the latter is included with the Supplementary Material (SM). This larger-scale preparation provided

TABLE I
Eluting System Used in TLC Measurement

	CH_2Cl_2 (V%)	Ethyl acetate (V%)
Zr(adsp)(dsp)	90	10
Zr(adsp)(mdsp)	80 ($CHCl_3$)	20
Zr(adsp) (cdsp)	88	12
Zr(adsp)(3-OCH_3dsp)	85	15
Zr(adsp)(5-OCH_3dsp)	80	20

sufficient quantity of solution to permit subdivision into six portions and subsequent reaction of five of these six (see below).

Attempts to append functionalized Zr(adsp)(Rdsp) groups onto the Kapton-like nonpendent co-PAA by use of the method previously described for R = H,[54] resulted in solvent-swollen gels being formed, often before the 1 : 1 mole ratio addition of dicyclohexylcarbodiimide (DCC) was completed. Because this gel formation interfered with the attachment of the desired concentration of pendent groups, subsequent workup, and/or characterization, results for these products are not included.

co-Poly[(4,4′-oxydiphthalic anhydride/3,4′-oxydianiline)$_{0.9}${mellitic acid dianhydride/3,4′-oxydianiline-*p*-((4-amino-*N*,*N*′-disalicylidene-1,2-phenylenediaminato)(functionalized *N*,*N*′-disalicylidene-1,2-phenylenediaminato)zirconium (IV))}$_{0.1}$]amic acid, co-PAA[(OPDA/3,4′-ODA)$_{0.9}${MADA/3,4′-ODA-*p*-Zr(adsp)(Rdsp)}$_{0.1}$]

The aforementioned freshly prepared, large-scale co-PAA solution was separated into six equal portions, and each portion (containing 6 mmol of 3,4′-ODA, 5.4 mmol of ODPA, and 0.6 mmol of MADA) was transferred to a separate 100-mL round-bottom flask. To achieve a 1 : 1 mole ratio of Zr(adsp)(Rdsp) to MADA, 0.6 mmol batches of the five different Zr(adsp)(Rdsp) complexes were separately dissolved in dried NMP. Each of the resulting Zr(adsp)(Rdsp) solutions was then mixed well with its own portion of co-PAA solution, leaving one portion of co-PAA solution for other use. Appending reactions were then conducted as described for Zr(adsp)(Rdsp) with R = H,[52–54] with very slow addition of DCC to avoid gel formation. TLC tests were performed on each using the eluent solutions given in Table I to confirm that no free zirconium complex remained.

One-milliliter portions of the nonpendent co-PAA and each of the pendent co-PAA solutions were separately added into a blender with stirring anhydrous ether. After filtering and washing with anhydrous ether, solid polymer powder was obtained. The six different polymers were then dried in a vacuum desiccator at room temperature for at least 2 days until constant weight was reached. Because significant amounts of NMP remained after various attempts to remove it, as indicated by proton NMR and elemental analysis, calculation of percent yield was not performed.

co-Poly[(4,4′-oxydiphthalic anhydride/3,4′-oxydianiline)$_{0.9}${mellitic acid dianhydride/3,4′-oxydianiline-*p*-((4-amino-*N*,*N*′-disalicylidene-1,2-phenylenediaminato)(functionalized *N*,*N*′-disalicylidene-1,2-phenylenediaminato)zirconium (IV))}$_{0.1}$]imide, co-PI[(OPDA/3,4′-ODA)$_{0.9}${MADA/3,4′-ODA-*p*-Zr(adsp)(Rdsp)}$_{0.1}$]

To induce imidization, co-PAA[(OPDA/3,4′-ODA)$_{0.9}${MADA/3,4′-ODA-*p*-Zr(adsp)(Rdsp)}$_{0.1}$] films and powder samples were heated in the manner described previously.[52–54] After heating, the films were still transparent, but their colors were more intense, ranging from yellow (R = H, methyl, CN) to yellow-orange (R = 3-methoxy, 5-methoxy), and appearing more orange with increasing thickness.

RESULTS AND DISCUSSION

Subdivision of the nonpendent co-PAA solution before appending the Zr(adsp)(Rdsp) components insured that the polymer average chain lengths would be the same for each *pendent* co-PAA and that any difference in properties would be due to the pendent group functionalities. As observed in the TLCs of co-PAA appending reaction solutions with unsubstituted Zr(adsp)(dsp),[52–54] the disappearance of the free complex spot upon addition of a sufficient amount of DCC and the acquisition of the complex's color by the polymer's spot were good indications that the expected appending reactions had occurred.

Polymer characterization

Structural

Proton NMR and FTIR spectral data for the new pendent co-PAAs and pendent co-PIs, respectively, along with the data for the corresponding nonpendent and nonfunctionalized pendent polymers, are collected in Table II. Imidization rendered the pendent co-PIs too insoluble for NMR, and the abundance of residual NMP (an amide itself) in the pendent co-PAA samples obscured significant regions of their FTIRs, so these data are not included. The key NMR features for the new pendent co-PAAs corresponded to those for the unsubstituted pendent co-PAA,[52–54] i.e., the appearance of amide proton signals approximately 10 ppm consisting of a large singlet due to ODPA/3,4′-ODA and two much smaller singlets attributed to meta- and para- attachments of MADA/3,4′-ODA, the

TABLE II
IR and NMR Data for Functionalized Zr-Pendent co-PAAs and co-PIs, and Related Polymers and Compounds

IR data for co-PIs (cm^{-1})

Sample	C—H	CN (cyano)	C=O (anh)[a]	C=O (imide)	C=C (aromatic)	C—N	C—O	C—H bending
co-PI	3073		1851	1779, 1720	1606	1376	1276 (anh)[a]	744
co-PI/Zr(H)	3071, 2932, 2857			1778, 1723	1607, 1542	1376	1248	748
co-PI/Zr(m)	3071, 2935, 2858			1780, 1725	1607, 1542	1376	1246	748
co-PI/Zr(c)	3072, 2932, 2858	2227		1778, 1724	1607, 1544	1376	1246	748
co-PI/Zr (3-OCH_3)	3072, 2931, 2860			1780, 1724	1607, 1544	1375	1247	746
co-PI/Zr (5-OCH_3)	3072, 2933, 2856			1778, 1724	1607, 1543	1375	1247	747

Proton NMR data (ppm, d^6-DMSO, integration in parentheses)

Sample	Amide	Imine (from complex)	Aromatic	Upfield shifted aromatic and amino (from complex)
co-PAA	10.87–10.86 (13.1)		8.19–6.27 (95.0)	
Zr (H)[b]		8.95–8.37 (10.2)	7.48–6.29 (48.2)	6.01–5.25 (13.9)
co-PAA/Zr (H)	11.00–10.12 (3.7)	8.92–8.33 (0.65)	8.23–6.16 (29.4)	6.02–5.45 (0.78)
Zr (m)[b]		8.7–8.3 (8.0)	7.4–6.3 (34.9)	5.8–5.3 (13.4)
co-PAA/Zr (m)	10.90–10.30 (3.7)	8.92–8.31 (0.66)	8.24–6.15 (30.5)	6.01–5.44 (0.78)
Zr (c)[b]		8.93–8.22 (10.7)	8.20–6.07 (50.3)	6.02–5.09 (16.3)
co-PAA/Zr (c)	10.94–10.15 (4.0)	8.96–8.46 (0.53)	8.18–6.27 (30.7)	6.00–5.60 (0.41)
Zr/(3-OCH_3)[b]		8.9–8.2 (8.3)		7.89–4.98 (50.2)
co-PAA/Zr (3-OCH_3)	10.88–10.18 (4.0)	8.84–8.48 (0.38)	8.17–6.19 (33.2)	
Zr/(5-OCH_3)[a]		8.95–8.43 (5.7)	7.85–6.36 (24.7)	6.07–5.37 (8.6)
co-PAA/Zr (5-OCH_3)	10.98–10.22 (3.9)	8.88–8.37 (0.62)	8.37–6.45 (28.8)	5.93–5.59 (0.39)

[a] anh = anhydride ring.
[b] Data collected in this work, agrees with Ref. 57.

observation of small singlets around 8.7 from the imine protons of the complexes, and the appearance of small multiplets due to upfield shifted aromatic protons from the complex.[59–61] The integrations were consistent with the 1 : 9 mole ratio of pendent and nonpendent mer units. The aliphatic signals expected for the methyl and methoxy groups were obscured by larger solvent signals. The presence of the electron-withdrawing cyano group was indicated by the downfield shift of signals from the adjacent aromatic protons resolving them from the aromatic signals of the polymer backbone. As expected, the FTIR spectra of the new pendent co-PIs did not show any peaks near 1850 cm^{-1} indicating that pendent group attachment once again was preventing anhydride ring formation.[52–54] Small peaks around 2900 cm^{-1} attributed to imine C–H stretching and around 1535 cm^{-1} attributed to aromatic C–H stretching were resolved from the stronger peaks from the polymer backbone and were consistent with the complexes being present. While signals from the other functional group vibrations were masked, a small peak at 2220 cm^{-1} was attributed to the presence of a cyano group for co-PI[$(OPDA/3,4'\text{-}ODA)_{0.9}$ {MADA/3,4′-ODA-p-Zr(adsp)(CNdsp)}$_{0.1}$].

The GPC results of nonpendent and zirconium pendent co-PAAs are shown in Table III and in SM Figures 1–6. All of the samples showed high average molecular weights for step growth polymers. These molecular weights are rough approximations because of the use of polystyrene standards, which have very different structures from the co-PAAs being analyzed. Because a universal calibration curve was used (based on hydrodynamic volume rather than MW of the standards), the molecular weights calculated are considered absolute molecular weights independent of the standards used. Because MADA has a slightly greater reactivity than ODPA,[53] it is expected that some polymer chains have more MADA units than others. The MADA-rich chains acquired more of the pendent groups than the MADA-poor ones, resulting in increased polydispersity for the pendent polymers.[52–54]

The different functional substituents used caused a significant scatter in the intrinsic viscosities (IV) and polydispersities. co-PAAs with methoxy groups gave the largest values for each, regardless of substituent location (3- or 5-). This finding may be indicative of the effect of these functional groups on the hydrodynamic volumes of these materials. The

TABLE III
GPC Results for Nonpendent and Zirconium Pendent co-PAAs

Sample	M_n (g/mol^{-1})	M_w (g/mol^{-1})	M_z (g/mol^{-1})	Intrinsic viscosity (dL/g^{-1})	Polydispersity (M_w/M_n)	Polydispersity (M_z/M_w)
co-PAA	4160	39200	64300	0.375	9.40	1.64
	3990	37400	61600	0.378		
co-PAA/Zr(H)	3100	118300	226700	0.459	38.40	1.93
	2910	112500	219200	0.465		
co-PAA/Zr(m)	5260	86600	159100	0.273	15.89	1.84
	5500	84400	155600	0.277		
co-PAA/Zr(c)	3220	104400	205800	0.410	33.38	1.96
	3090	106200	206600	0.508		
co-PAA/Zr(3-OCH_3)	1970	123400	249200	0.647	64.23	2.02
	1910	125700	254300	0.663		
co-PAA/Zr(5-OCH_3)	1870	183200	450600	0.581	94.39	2.45
	1980	180200	439500	0.566		

greater observed average Mw for the 5-methoxy pendent co-PAA vs. those with other substituents could be attributable to the presence of two methoxy groups on each pendent and their outwardly disposed orientation.

Thermal

TGA was used to determine the thermal stability of co-PAAs and co-PIs with and without zirconium pendent groups. The approximate mole percentage of pendent groups present was confirmed via the amount of ZrO_2 residue produced upon the thermal decomposition in air.[54] SM Figures 7 and 8–12 show the TGA graphs of the nonpendent co-PAA and corresponding Zr(adsp)(Rdsp) pendent co-PAAs, respectively. In all cases two stages of weight loss are seen, attributed to an imidization step and a decomposition step. Table IV summaries the results obtained from these TGA graphs.

The table shows that both nonpendent and zirconium pendent polymers had approximately the same imidization temperature and that the zirconium pendent polymers had lower thermal stabilities as anticipated[52–54] but comparable with LARC-IA.[56] The co-PIs with functional substituents on the pendent groups had thermal stabilities 5–28°C lower than that of the unsubstituted pendent co-PI. The methoxy functionality in the 3-position on the salicylidene rings produced the smallest decrease of the functional groups tested, most likely due to its less exposed orientation. However, because all the thermal decomposition temperatures remained above 500°C, the thermal stabilities of the new polymers were still considered to be very high.

Typical DSC curves of heat flow versus temperature for nonpendent and pendent co-PI samples are shown in SM Figures 13 and 14–18, respectively. All samples were analyzed twice. There was generally one endothermic peak in the first scan for each. The glass transition temperatures, T_gs, from the first analysis were lower than those from the second. Additional curing and/or the onset of crosslinking are likely to be contributing to the observed increase in T_gs. "Fresh" polymer is used to measure T_g because it is a time-related parameter. T_gs for all of the imidized films are listed in Table V. The absence of endotherms associated with melting temperatures, T_m, indicated a lack of crystalline behavior in these co-PIs. For the co-PAA films, only solvent evaporation curves were observed when the heating cycle was kept below the temperature corresponding to the onset of imidization so their T_gs could not be determined.

Upon comparing the T_gs of nonpendent and zirconium pendent co-PIs with that of LARC-IA, which is 223°C,[56] those of the co-PIs synthesized in this research were much higher. The structural difference between the nonpendent co-PI and LARC-IA is the

TABLE IV
TGA Results for Nonpendent co-PAA and Zirconium Pendent co-PAAs

Sample	Imidization (°C) Onset	Imidization (°C) Midpoint	Imidization (°C) Offset	Thermal decomposition (°C) Onset	Thermal decomposition (°C) Midpoint	Thermal decomposition (°C) Offset
co-PAA	137.6	171.3	204.6	583.4	612.0	642.0
co-PAA/Zr(adsp)(dsp)	138.0	174.9	210.6	551.5	582.3	613.9
co-PAA/Zr(adsp)(mdsp)	136.2	167.2	199.4	521.3	554.3	592.1
co-PAA/Zr(adsp)(cdsp)	136.8	170.7	204.1	535.7	568.4	607.6
co-PAA/Zr(adsp) (3-OCH_3dsp)	133.7	169.9	205.7	547.8	576.5	604.5
co-PAA/Zr(adsp) (5-OCH_3dsp)	133.9	166.7	199.5	529.3	560.8	594.7

TABLE V
Glass Transition Temperatures from DSC Results for co-PI Films

Sample	First heating circle (°C)			Second heating circle (°C)		
	Onset	Midpoint	Offset	Onset	Midpoint	Offset
co-PI	230.8	234.4	239.0	252.2	255.7	260.0
co-PI/Zr(adsp)(dsp)	229.7	236.4	242.6	296.0	319.8	328.8
co-PI/Zr(adsp)(mdsp)	229.4	238.4	253.2	307.1	319.2	329.3
co-PI/Zr(adsp)(cdsp)	235.0	248.2	254.4	287.4	304.8	313.4
co-PI/Zr(adsp) (3-OCH_3dsp)	235.2	255.1	257.5	276.1	287.1	291.1
co-PI/Zr(adsp) (5-OCH_3dsp)	239.1	255.2	260.4	292.3	312.2	315.5

presence of MADA in the former. Because of the rigidity of MADA, the flexibility of the polymer backbone is less causing the T_g to be greater.[52–54] Comparing zirconium pendent co-PIs to nonpendent co-PI, the immobilizing effect of the massive zirconium complexes also cause T_gs to be higher.[52–54] Upon comparison to the nonfunctionalized Zr pendent polymer, all of the functionalized Zr pendent co-PIs had higher T_gs in the first run by 2–19°C, but had lower midpoints in the second run by 0.6–32°C. The implication of this result is that additional attractions caused by the functional groups lessen polymer chain mobility in the first run, but interfere with the efficiency of polymer chain packing in the second run. The Zr pendent co-PI with methyl substituents underwent the smallest change of T_g (+2°C) and those with 3- or 5-methoxy substituents underwent the largest change of T_g (+19°C) from that of the non-functionalized pendent co-PI, which is in parallel with their impacts on IV and polydispersity values from GPC (Table III). Recall that 3-methoxy substituents had the *least* effect on thermal stability. If enhanced polymer chain interactions are responsible for the higher midpoints in the second DSC runs, then the 3-methoxy substituents are the most effective of the functional groups studied at suppressing these interactions (an increase of only 32°C from its first run midpoint vs. increases of 56–81°C for the other functionalized Zr pendent co-PIs). At 287.1°C, the midpoint of the second heating cycle for the 3-methoxy Zr co-PI is the lowest of the functionalized Zr co-PIs, and is 32°C lower than that of the unsubstituted Zr co-PI. It should be noted that the 3-methoxy groups are the only substituents in this study to be oriented toward the polymer backbone. While the 5-methoxy co-PI was tied with the 3-methoxy co-PI for the largest effect on the T_g in the first run (+19°C), it produced the second smallest change in the midpoint of the second run vs. that of the unsubstituted Zr co-PI (–8°C).

Light scattering

Light scattering is a tool that has been used to reveal the extent of polymer chain aggregation in solution, which in turn provides insight into the strength of polymer chain interaction vs. polymer chain-solvent interaction.[6,25] Weight average molecular weight is the only molecular weight that can be obtained from these experiments. SM Figure 19 shows R_{90}/K_c (g/mol) vs. c (g/cc) for nonpendent and Zr-pendent co-PAAs. Table VI shows the light scattering results. Note the low second virial coefficient for the co-PAA/Zr(adsp)(cdsp) and the corresponding high weight average molecular weight vs. the other Zr-pendent co-PAAs tested.

When the second virial coefficient is low, the interaction between polymer and solvent is poor. Therefore, aggregation may occur when this value is low. Because the second virial coefficient of Zr(adsp)(cdsp) pendent co-PAA was about half that of the other co-PAAs in this study, and the average molecular weight was about double, formation of aggregates with an average of two polymer chains apiece appears to have occurred.

Because the average molecular weight of Zr(adsp)(cdsp) pendent co-PAA was not double that of the other substituted Zr-pendent co-PAAs obtained from GPC, our initial interpretation was that addition of 0.02 M LiBr to the NMP was effective at suppressing the aggregation. However, it was also noted that the GPC average M_ws for the unsubstituted, 3-methoxy, and 5-methoxy Zr pendent co-PAAs were approximately double those obtained by light scattering, unlike the values for the nonpendent co-PAA. Therefore, an alternate interpretation is

TABLE VI
Light Scattering Results for Nonpendent and Zirconium Pendent co-PAAs

Sample	M_w (g/mol) × 10^4	A2 (mol cm^{-3} g^{-2})
co-PAA	4.7	3.4
co-PAA/Zr(adsp)(dsp)	5.9	2.8
co-PAA/Zr(adsp)(mdsp)	7.4	2.6
co-PAA/Zr(adsp)(cdsp)	13	1.4
co-PAA/Zr(adsp) (3-OCH_3dsp)	6.9	3.1
co-PAA/Zr(adsp) (5-OCH_3dsp)	7.4	2.3

TABLE VII
Results of Contact Angle Measurement for Nonpendent and Zirconium Pendent co-PAAs

Sample	Contact angle
co-PI	58.8
co-PI/Zr(adsp)(dsp)	60.8
co-PI/Zr(adsp)(mdsp)	58.7
co-PI/Zr(adsp)(cdsp)	60.5
co-PI/Zr(adsp) (3-OCH_3dsp)	60.8
co-PI/Zr(adsp) (5-OCH_3dsp)	60.7
LARC-IA[a]	62.7
LARC-IA[b]	62.6

[a] LARC-IA film was made at 360°C, 10T.
[b] LARC-IA film was made at 340°C, 5T.

that, at 60°C, aggregation occurs for all of the functionalized Zr pendent PAAs (with ca. $n = 2$, somewhat less for methyl); and that only the cyano functionalized Zr pendent co-PAA is aggregated at room temperature, which is the temperature of the sample solutions in the light scattering experiment and the temperature at which films were cast (see next section). Labilization of dsp(2-) ligands in the Zr pendent groups resulting in disproportionation (i.e., a crosslinked site and a free Zr complex),[49] is one mechanism by which aggregation could be occurring.

Film properties

Films of Zr(adsp)(cdsp) pendent co-PI, cast from NMP solution and thermally imidized, far surpassed those of the other substituted Zr pendent co-PIs in film quality and resistance to cracking. This property is attributed to the room temperature aggregation noted previously, which allowed the corresponding co-PAA to behave as if it had twice the average molecular weight compared to the others. Because aggregates behave like large polymers, it is no surprise that the Zr(adsp)(cdsp) pendent polymer provided the best films. After immersion in acetone, chloroform, dimethylacetamide (DMAc), methyl ethyl ketone, and toluene for 30 min, each co-PI film sample remained flexible and passed the fingernail crease test comparable to the corresponding untreated films. The fact that treatment with different organic solvents caused no changes in the films indicated that no dissolution of low molecular weight polymer occurred. Compared with LARC-IA,[56] enhanced solvent resistance was observed for nonpendent co-PI and zirconium pendent co-PI films, presumably because of the presence of rigid MADA residues in the polymer chain. Upon preparing 2-layer zirconium pendent co-PI films, cracks were apparent after imidization. Attachment of the zirconium complex may reduce the flexibility of the polymer chains, which would cause adhesion of the polymer films to the glass substrate to be weaker; or, for material not adjacent to the glass, the greater difference in Thermal Coefficients of Expansion between Zr pendent co-PAA and co-PI, vs. nonpendent co-PAA and co-PI, may be causing cracks to form.

Contact angle measurement was performed to check the surface properties of parent polyimide film, zirconium pendent polyimide films, and LARC-IA films. Table VII shows the result of contact angle measurement.

The incorporation of MADA moieties into the LARC-IA structure seems to enhance the surface affinity for water, causing the applied drop to spread out more, and subsequent reaction at the MADA locations seems to diminish that enhancement. Based on these contact angle measurements the potential for use of these pendent polymers as adhesives is good.

Upon exposing each film to atomic oxygen via plasma etching, chalky white residue appeared on the surface of the zirconium pendent co-PI films, but not the nonpendent co-PI films. The formation of chalky residue was attributed to the decomposition of attached zirconium complexes to ZrO_2.[52–54] The surface appearance of nonpendent co-PI and zirconium pendent co-PI films before and after oxygen plasma etching for three hours were recorded by scanning electron microscopy; see SM Figures 20–22. After AO exposure, all of the pendent polyimide films were more pitted than the nonpendent polyimide film (less so for the Zr(adsp)(5-OCH_3dsp) co-PI), presumably due to increased porosity. Progress toward increasing the aerial density of Zr in similar pendent co-PIs is described in the next article in this series.[52]

CONCLUSIONS

Evidence is presented that four new functionalized Zr pendent co-PAAs and the corresponding co-PIs have been prepared with reasonably high average molecular weights for step growth polymers, i.e., co-PAA[(OPDA/3,4′-ODA)$_{0.9}${MADA/3,4′-ODA-*p*-Zr(adsp)(Rdsp)}$_{0.1}$] and co-PI[(OPDA/3,4′-ODA)$_{0.9}$ {MADA/3,4′-ODA-*p*-Zr(adsp)(Rdsp)}$_{0.1}$], where R = 3-methoxy or 5-methoxy on the salicylidene rings, or 5-cyano (nitrile) or 5-methyl on the diamine ring. Functionalizing the Zr pendent groups even at the relatively low concentration of 10 mole percent caused significant changes in polymer properties such as aggregation in NMP, T_gs, and film quality. The implication is that more can be done with functional group content to fine-tune polymer chain interactions.

References

1. Hao, X.; Heuts, J. P. A.; Barner-Kowollik, C.; Davis, T. P.; Evans, E. J Polym Sci Part A: Polym Chem 2003, 41, 2949.

2. Varshney, V.; Carri, G. A. J Chem Phys 2007, 126, 044906/1.
3. Percec, V.; Cho, W.-D.; Ahn, C.-H.; Schlueter, D.; Johansson, G.; Mosier, P. E.; Ungar, G.; Moller, M.; Sheiko, S. S.; Hudson, S. D.; Jung, H.-T. Polym Mater Sci Eng 1997, 77, 97.
4. Percec, V.; Johansson, G.; Schlueter, D.; Ronda, J. C.; Ungar, G. Macromol Symp 1996, 101, 43.
5. Sferrazza, M.; Jones, R. A. L.; Penfold, J.; Bucknall, D. B.; Webster, J. R. P. J Mater Chem 2000, 10, 127.
6. Nguyen, T.-Q.; Doan, V.; Schwartz, B. J. J Chem Phys 1999, 110, 4068.
7. Nguyen, T.-Q.; Martini, I. B.; Liu, J.; Schwartz, B. J. J Phys Chem B 2000, 104, 237.
8. Stribeck, N.; Wutz, C. Macromol Chem Phys 2002, 203, 328.
9. Kim, J. Pure Appl Chem 2002, 74, 2031.
10. Berggren, M.; Bergman, P.; Fagerstrom, J.; Inganas, O.; Andersson, M.; Weman, H.; Granstrom, M.; Stafstrom, S.; Wennerstrom, O.; Hjertberg, T. Chem Phys Lett 1999, 304, 84.
11. Nanasawa, A.; Takayama, S.; Takeda, K. J Appl Polym Sci 1997, 66, 2269.
12. Ilhan, F.; Gray, M.; Blanchette, K.; Rotello, V. M. Macromolecules 1999, 32, 6159.
13. Hamilton, A. N.; Middaugh, J. D. In 17th Proceedings of the Electrical/Electrical Insulation Conference; Institute of Electrical & Electronic Engineers (IEEE): New York, 1985; p 68.
14. Chang, M. H.; Frampton, M. J.; Anderson, H. L.; Herz, L. M. Phys Rev Lett 2007, 98, 027402.
15. Xu, H.; Shenhar, R.; Hong, R.; Srivastava, S.; Rotello, V. M. Polym Mater Sci Eng 2007, 96, 933.
16. Wu, S.-C.; Shu, C.-F. J Polym Sci Part A: Polym Chem 2003, 41, 1160.
17. Huang, E.; Rockford, L.; Tussell, T. P.; Hawker, C. J. Nature (London) 1998, 395, 757.
18. Erukhimovich, I.; Abetz, V.; Stadler, R. Macromolecules 1997, 30, 7435.
19. Yamaguchi, A.; Ohta, M. In International SAMPE Technical Conference; Hoggatt, J. T., Hill, S. G., Johnson, J. C., Eds.; Society for the Advancement of Material Process Engineering (SAMPE): Covina, California, 1986; Vol. 18, p 229.
20. Kimishima, K.; Jinnai, H.; Hashimoto, T. Macromolecules 1999, 32, 2585.
21. Schubert, U. S.; Nuyken, O.; Hochwimmer, G. J Macromol Sci Pure Appl Chem 2000, A37, 645.
22. Schwartz, B. J. Ann Rev Phys Chem 2003, 54, 141.
23. Bassmann, F. Ber des Forschungszentrums Juelich, Juel-3975; 2002; Vol. i–xiii, p 1.
24. Nguyen, T.-Q.; Schwartz, B. J. J Chem Phys 2002, 116, 8198.
25. Qiu, X.; Kwan, C. M. S.; Wu, C. Macromolecules 1997, 30, 6090.
26. Le Fevere De Ten Hove, C.; Penelle, J.; Ivanov, D. A.; Jonas, A. M. Nat Mater 2004, 3, 33.
27. Rastello De Boisseson, M.; Leonard, M.; Hubert, P.; Marchal, P.; Stequert, A.; Castel, C.; Favre, E.; Dellacherie, E. J Colloid Interface Sci 2004, 273, 131.
28. Amrutha, S. R.; Jayakannan, M. J Phys Chem B 2006, 110, 4083.
29. Amrutha, S. R.; Jayakannan, M. Macromolecules 2007, 40, 2380.
30. Hao, X. T.; Hosokai, T.; Mitsuo, N.; Kera, S.; Okudaira, K. K.; Mase, K.; Ueno, N. J Phys Chem B 2007, 111, 10365.
31. McQuade, D. T.; Kim, J.; Swager, T. M. J Am Chem Soc 2000, 122, 5885.
32. Xu, B.; Zhang, J.; Peng, Z. Synth Met 2000, 113, 35.
33. Chiavarone, L.; Di Terlizzi, M.; Scamarcio, G.; Babudri, F.; Farinola, G. M.; Naso, F. Appl Phys Lett 1999, 75, 2053.
34. Liu, X.; Xu, W.; Ye, G.; Gu, Y. Polym Eng Sci 2006, 46, 123.
35. Shenhar, R.; Sanyal, A.; Uzun, O.; Rotello, V. M. Macromolecules 2004, 37, 92.
36. Kim, E. J.; Park, O. O. K. Mol Cryst Liq Cryst Sci Technol Sect A 1995, 267, 41.
37. Balagurusamy, V. S. K.; Ungar, G.; Percec, V.; Johansson, G. J Am Chem Soc 1997, 119, 1539.
38. Gasilova, E. R.; Shevelev, V. A.; Ivanova, V. N.; Bitsenko, M. I. Vysokomol Soedin 1995, 37, 2013.
39. Nguyen, T.-Q.; Kwong, R. C.; Thompson, M. E.; Schwartz, B. J. Synth Met 2001, 119, 523.
40. Nguyen, T.-Q.; Kwong, R. C.; Thompson, M. E.; Schwartz, B. J. Appl Phys Lett 2000, 76, 2454.
41. Cooke, G.; Couet, J.; Garety, J. F.; Ma, C.-Q.; Mabruk, S.; Rabani, G.; Rotello, V. M.; Sindelar, V.; Woisel, P. Tetrahedron Lett 2006, 47, 3763.
42. Eastwood, E.; Viswanathan, S.; O'Brien, C. P.; Kumar, D.; Dadmun, M. D. Polymer 2005, 46, 3957.
43. Rotello, V. M. Polym Prepr (Am Chem Soc Div Polym Chem) 2005, 46, 1148.
44. Shenhar, R.; Sanyal, A.; Uzun, O.; Nakade, H.; Rotello, V. M. Macromolecules 2004, 37, 4931.
45. Chang, M.-J.; Wang, Y.-M.; Yang, W.-T.; Jiang, G. J. Polym Prepr (Am Chem Soc Div Polym Chem) 2006, 47, 718.
46. Zhang, J.; Tsuji, H.; Noda, I.; Ozaki, Y. J Phys Chem B 2004, 108, 11514.
47. Viswanathan, S.; Dadmun, M. D. J Polym Sci Part B: Polym Phys 2004, 42, 1010.
48. Matsumoto, A. Polym J (Tokyo, Jpn) 2003, 35, 93.
49. He, L.; Wagner, S. R.; Illingsworth, M. L.; Yap, G. A.; Rheingold, A. L. Chem Mater 1997, 9, 3005.
50. Illingsworth, M. L.; Betancourt, J. A.; He, L. Chen, Y.; Terschak, J. A.; Banks, B. A.; Rutledge, S. K.; Cales, M. Zr-Containing 4,4′-ODA/PMDA Polyimide Composites, NASA Technical Memo, 2001–211099; NASA: Washington, DC, 2001; p 1.
51. Illingsworth, M. L.; Banks, B. A.; Smith, J. W.; Jayne, D.; Garlick, R. G.; Rutledge, S. K.; de Groh, K. K. Plasma Chem Plasma Proc 1996, 16, 209.
52. Chow, D.; Cheng, W.; Dai, H.; Siochi, E. J.; Wagner, S. R.; Luzzi, S. D.; Landi, B. J.; He, L.; Illingsworth, M. L. High Perform Polym, to appear.
53. Illingsworth, M. L.; Dai, H.; Wang, W.; Chow, D.; Siochi, E.; Yang, K.; Leiston-Belanger, J. M.; Jankauskas, J. J Polym Sci Part A: Polym Chem 2007, 45, 1641.
54. Wagner, S.; Dai, H.; Stapleton, R. A.; Siochi, E. J.; Illingsworth, M. L. High Perform Polym 2006, 18, 399.
55. Crosby, G. A.; Kato, M. J Am Chem Soc 1977, 99, 278.
56. Hou, T. H.; Johnston, N. J.; St. Clair, T. L. High Perform Polym 1995, 7, 105.
57. Illingsworth, M. L.; Wang, W.; Hughes, K. A.; Terschak, J. A.; McCarney, J. P.; Stapleton, R. A.; Wagner, S. R.; Trotter, K. J.; Courtney, R. E.; Giacofei, R. A.; Jensen, A. J.; Moisa, M. S.; Browning, T. A.; Puchebner, B. E.; Theimer, C. A.; Chen, Y. Syn React Inorg Met-Org Chem 2004, 34, 593.
58. Hiemenz, P. C. Principles of Colloid and Surface Chemistry; Marcel Dekker: New York, 1986.
59. Archer, R. D.; Day, R. O.; Illingsworth, M. L. Inorg Chem 1979, 18, 2908.
60. Illingsworth, M. L.; Cleary, B. P.; Jensen, A. J.; Schwartz, L. J.; Rheingold, A. L. Inorg Chim Acta 1993, 207, 147.
61. Illingsworth, M. L.; Rheingold, A. L. Inorg Chem 1987, 26, 4312.